Instabilities and Solitons in Minimal Strips

Thomas Machon,[1] Gareth P. Alexander,[1] Raymond E. Goldstein,[2] and Adriana I. Pesci[2]
[1]Department of Physics and Centre for Complexity Science, University of Warwick, Coventry CV4 7AL, United Kingdom
[2]Department of Applied Mathematics and Theoretical Physics, Centre for Mathematical Sciences, University of Cambridge, Wilberforce Road, Cambridge CB3 0WA, United Kingdom
(Received 8 February 2016; published 1 July 2016)

We show that highly twisted minimal strips can undergo a nonsingular transition, unlike the singular transitions seen in the Möbius strip and the catenoid. If the strip is nonorientable, this transition is topologically frustrated, and the resulting surface contains a helicoidal defect. Through a controlled analytic approximation, the system can be mapped onto a scalar ϕ^4 theory on a nonorientable line bundle over the circle, where the defect becomes a topologically protected kink soliton or domain wall, thus establishing their existence in minimal surfaces. Demonstrations with soap films confirm these results and show how the position of the defect can be controlled through boundary deformation.

DOI: 10.1103/PhysRevLett.117.017801

Minimal surfaces, critical points of the area functional, are geometric motifs that appear throughout physics. From their early identification in soap films [1], they have since been observed in a great variety of areas ranging from condensed matter [2] and biological physics to field theory. These involve the structure of boundaries in bicontinuous phases [3,4], smectic liquid crystals [5,6], membranes and tissues [7,8], and monopoles and twistor theory [9,10]. The simplest minimal surface is the plane, which is also the only stable complete minimal surface [11], and thus any other soap film surface must become unstable if the boundary is deformed beyond a critical conformation. Studies of these instabilities in soap film annuli have typically focused on the catenoid [12,13] and, more recently, the Möbius strip [14–16]. In both of these cases, as the boundary wire is varied, one sees an instability that leads to a singularity and subsequent topological change in the surface—to two discs in the case of the catenoid and a single disc in the case of the Möbius strip. More generally, these instabilities illustrate how surface tension serves to control morphology, and morphological changes, in a simple but generic system.

Here, we discuss instabilities in highly twisted minimal strips. We demonstrate that the collapsing instabilities observed for the catenoid and Möbius strip do not extend to an arbitrary number of twists. Instead, what is observed are buckling instabilities that lead to nonsingular transitions in the surface—similar in nature to the nonsingular "headphone" transitions studied by Courant [17]—and to the creation of ribbonlike structures analogous to those seen in the helicoid [18]. In geometric terms, the change in the morphology of the strip is from twist to writhe. We show that if the strip is nonorientable, the instability is topologically frustrated, and the resulting ribbon contains a topological defect or domain wall; this is visualized in a series of demonstrations with soap films. The simplest examples of domain walls are found in one-dimensional systems with two ground states such as polyacetylene [19–21] and its mechanical analogues [22,23], where the continuum limit is a ϕ^4 field theory [24,25]. By mapping the structure of the nonorientable strip onto such a theory, we show that these domain walls can be described as $\mathbb{Z}_2$ kink solitons, topologically protected by the nonorientability of the surface. The problem of how different minimal surfaces dynamically interconvert is currently poorly understood. The present work establishes perhaps the simplest observable example of this, and by mapping it onto a well-known field theory, a range of questions about the dynamics of such processes will become accessible.

The instabilities of a soap film are found by studying the second variation of area, since the energy derives entirely from surface tension. This leads to a Schrödinger operator with Dirichlet boundary conditions [26]

$$-\nabla^2 + 2K, \tag{1}$$

where K is the Gaussian curvature of the surface. The eigenfunctions of this operator correspond to the normal modes of a soap film realizing the particular surface, with the squared frequency, ω^2, given by the eigenvalues as $\lambda_i = dh\omega_i^2/\sigma$ where h, d, and σ are the thickness, density, and surface tension of the soap film, respectively [18]. For a physical soap film spanning a wire frame, any motion of the frame that pushes the lowest eigenvalue of (1) below zero will create an instability. It follows that an observed instability of a soap film must be both a solution of $(-\nabla^2 + 2K)\psi = 0$, known as a Jacobi field, and the ground state of (1).

The eigenfunction ψ represents an infinitesimal deformation of the surface in the normal direction: the mode of deformation at the point of instability. Its nature depends upon the topological type of the minimal strip, determined by an integer, q, equal to the number of half twists in the strip; the catenoid corresponds to $q = 0$ and the Möbius strip to $q = \pm 1$. Examples of surfaces with arbitrary q are given by the bent helicoids [27,28], shown in Fig. 2(c), which are determined by their Weierstrass data, $g(w) = -w(w^{q/2} + i)/(iw^{q/2} + 1)$ and $df = (2w)^{-1}(w^{q/2} + w^{-q/2})dw$, and contain the unit circle in the x-y plane. If q is odd the surface is nonorientable and orientable if q is even. They have q-fold rotational symmetry about their axial direction, and the geometry of the surfaces is pure twist with no writhe. From Bloch's theorem we know that, in terms of coordinates (u, v) with $w = 2(u + iv)/q$, where $u \in [0, q\pi)$ runs along the strip, ψ is of the form $\psi(u, v) = \psi_q(u, v)$ for an orientable strip, where $\psi_q(u, v) = \psi_q(u + \pi, v)$. If the surface is nonorientable, then the surface normal, $\mathbf{n}$, reverses sign upon traversal of the strip, meaning that ψ necessarily contains a nodal line which marks the position of the soliton. Equivalently, one requires antisymmetric boundary conditions and so ψ must be of the form $\psi(u, v) = \sin(u/q)\chi_q(u, v)$, where χ_q is a q-fold periodic function as in the orientable case.

While the functions ψ_q and χ_q have q-fold symmetry, because of the twisted nature of the circular helicoids, $\mathbf{n}$ has only $q/2$-fold rotational symmetry and reverses sign under a rotation of $2\pi/q$, that is

$$\mathbf{n}(u, v) = -\mathbf{n}(u + \pi, v). \tag{2}$$

Consequently, for $|q| > 1$, the instability pushes adjacent segments of the surface in opposite directions, as shown in Fig. 2(c), which leads to a buckling of the surface to form a ribbon, illustrated in Fig. 2, rather than the collapse that characterizes both the catenoid ($q = 0$) and Möbius strip ($|q| = 1$). In the nonorientable case, the nodal line in ψ means that the instability is frustrated. As such, when the nonorientable strip undergoes its instability, there is a helicoidal defect created in the ribbon surface, which one can think of as a local interpolation between two ribbon surfaces. This defect marks the location of a topological soliton in the soap film. The topological nature of the phenomenon means that it is robust to perturbations and deformations of the surface, or indeed the exact shape of the bounding frame: it is a generic feature of nonorientable minimal strips with multiple half twists ($|q| > 1$). We have realized examples with soap films on frames with circular axes, shown in Fig. 2(b), and also on the straight portion of frames resembling a hippodrome, shown in Fig. 1. The latter allows the defect to be studied in the straight region of the frame where the boundary is an ordinary straight double helix. This setting simplifies some of the analysis without sacrificing any features.

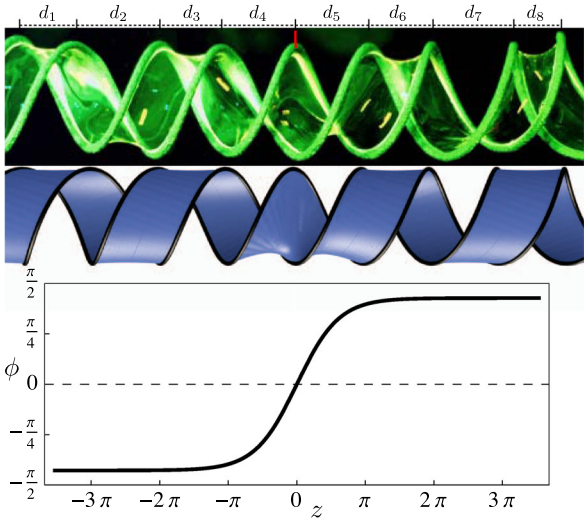

FIG. 1. Topological soliton on a soap film bound by a helical frame. *Top*: Photograph of the soliton on a soap film, marked with a red line, with helical boundary curves. Note that to the left of the soliton $d_{2n} > d_{2n\pm1}$, whereas to the right $d_{2n} < d_{2n\pm1}$, indicating a deformation of the boundary localizing the soliton. *Middle*: Plot of the ruled surface approximation with similar ρ to the photograph, with $\phi = m\tanh(\sqrt{2\lambda}mz)$. *Bottom*: Graph of the associated tanh solution for ϕ.

On the straight helical frame, the initial surface is the helicoid, whose instabilities have been studied by Boudaoud *et al.* [18]. The surface is given by $\Sigma(u, v) = (\sinh v \cos u, \sinh v \sin u, u)$, where $u \in \mathbb{R}$ and $\sinh v \in [-\rho, \rho]$. As ρ grows beyond a critical threshold, $\rho^* \approx 1.509$, this helicoid undergoes the aforementioned buckling instability to form a ribbon, shown in Fig. 2(a). This can result in one of two separate ribbons, depending on the sign of the initial instability [18], which are related to each other by a translation of half a period in the vertical direction. The transition changes the symmetries of the surfaces, whereas the helicoid has a translation symmetry of π in the vertical direction, the ribbon surfaces have the reduced translational symmetry of 2π, a consequence of the symmetries of the normal vector (2) and the form of the instability. If we take a vertical interval of π as an initial unit cell, then the instability in the helicoid can be thought of as a case of spatial period doubling, as in Peierls dimerization. The helical soliton we describe is then directly analogous to the solitons found in the Su-Schrieffer-Heeger (SSH) model [19–21] and is topologically protected if q, the number of unit cells, is odd.

The helicoid is simple enough that the Jacobi field can be found in both the orientable and nonorientable cases (see Supplemental Material [29]). For a helicoid in a periodic domain, $(x, y, z) \sim (x, y, z + q\pi)$ the Jacobi field in the orientable case is $\psi(u, v) = 1 - v\tanh v$ [18] (see Supplemental Material [29] also), and in the nonorientable case, where q is odd, it is $\sin(u/q)\chi_q(v)$, where

$$\chi_q(v) = Q_2^{1/q}(0)P_1^{1/q}(\tanh v) - P_2^{1/q}(0)Q_1^{1/q}(\tanh v), \tag{3}$$

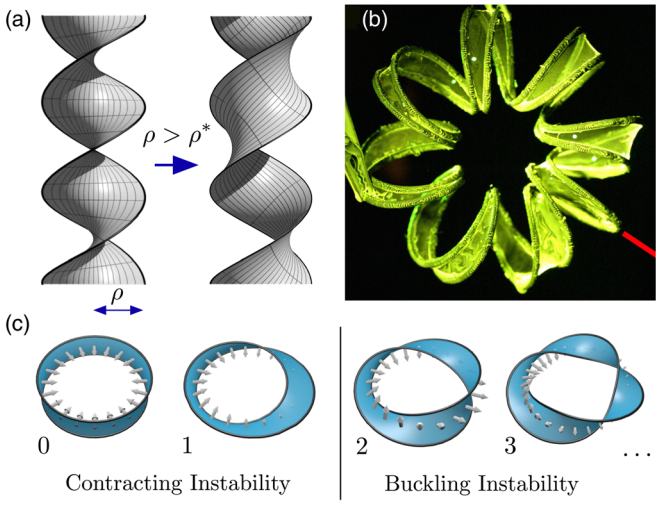

FIG. 2. (a): The instability in the helicoid. For $\rho < \rho^* \approx 1.509$, the helicoid is stable, but above this critical value there is an instability which leads to the formation of a ribbon, shown on the right. (b): Photograph of a soap film on a circular helix frame containing a kink soliton, indicated by a red line. The radius of the helix is sufficiently large that the buckling transition occurs and the ribbon is preferred over a circular helicoid. The boundary curve has an odd number half twists making the surface nonorientable and leading to the presence of the defect. At the defect the surface is locally helicoidal and can be thought of as interpolating between two ribbons that are π out of phase with each other. (c) Bent helicoids with $q = 0$, 1, 2, and 3 half twists. The arrows indicate the nature of the instability. For $|q| > 1$, the instability leads to a buckling transformation, rather than the collapse that occurs for $q = 0$, 1. If q is odd, then this buckling transition is frustrated, leading to the creation of a defect [shown in (b)].

and $P_n^m(x)$ and $Q_n^m(x)$ are the Legendre functions of the first and second kind, respectively. In the orientable case, the critical threshold $\rho^* \approx 1.509$ is determined by the zeros of $1 - v\tanh v$ and does not depend on q. In the nonorientable case, the critical value ρ_q^* depends on q and forms a decreasing sequence with limiting value ρ^*. Hence, for any finite q, $\rho_q^* > \rho^*$, and the corresponding nonorientable helicoid enjoys a slightly greater degree of stability than its orientable brethren.

We now turn to the shape of the soliton. In the orientable case, exact forms exist for the resulting ribbon surfaces [18], including those with a circular axis [27–29]. However, to find the form of the ribbon surface containing the topological defect, we turn to an approximation. Aside from the plane, the helicoid is well-known to be the only ruled minimal surface, and for ρ just above the critical value, the resulting ribbon is close in form to the helicoid. We therefore approximate the system by a set of ruled surfaces given by the formula

$$\Sigma(z, r) = rc_1(z - \phi(z)) + (1 - r)c_2(z + \phi(z)), \quad (4)$$

where $r \in [0,1]$, $z \in [0, q\pi)$, and the boundary curves are given by $c_1(z) = (\rho\cos z, \rho\sin z, z)$ and $c_2(z) = (-\rho\cos z, -\rho\sin z, z)$.

The surface (4) connects points on one helical boundary to the other by straight lines, offset by a phase of $2\phi(z)$, as illustrated by Fig. 3, where $\phi = 0$ corresponds (exactly) to the helicoid, and a constant value of $\phi \neq 0$ yields a ribbonlike surface. To test the validity of this approximation, we find the value of ϕ that minimizes the area functional

$$A = \int_0^{q\pi} \int_0^1 |\partial_z \Sigma \times \partial_r \Sigma| dr dz, \quad (5)$$

for a given boundary radius ρ (see Supplemental Material [29]). For small ρ, $\phi = 0$ gives the minimal solution as a helicoid. As in the general case, there is a pitchfork bifurcation at a finite value, $\bar{\rho}$, above which there are two nonzero equilibrium values $\pm\bar{\phi}(\rho)$. As ρ grows large $\bar{\phi} \to \pi/2$, corresponding to a ribbon surface lying on the surface of a cylinder of radius ρ. The transition radius $\bar{\rho} \approx 1.511$ is close to the value for the instability of the helicoid of $\rho^* \approx 1.509$ though necessarily slightly greater.

To study the shape of the soliton on the periodic helicoid, we must allow ϕ to vary. Just above the transition radius, $\bar{\rho}$, the equilibrium values $\pm\bar{\phi}$ are close to zero, allowing us to expand to low order in ϕ. Performing the r integration in (5), we find

$$A \approx \int \alpha + \beta\phi^2 + \gamma\phi^4 + \delta(\phi')^2 dz, \quad (6)$$

where the values of α, β, γ, and δ depend on ρ (see Supplemental Material [29]), and we have temporarily suppressed the limits on the integral. Equation (6) gives the spatial part of the Lagrangian for a scalar ϕ^4 theory on the circle [24,25], and ϕ may be thought of as analogous to the field u in the SSH model [19–21]. The helical defect, shown in Figs. 1 and 2, therefore corresponds to a kink soliton in the ϕ^4 theory in (6). In the periodic domain with q even, one has regular periodic boundary conditions, $\phi(z + q\pi) = \phi(z)$ and (6) has two ground state solutions, $\phi = \pm\bar{\phi}$. Kink solitons in the orientable case are then excitations of this ground state and must come in kink antikink pairs. In the nonorientable case, we have $\phi(z + q\pi) = -\phi(z)$, and the existence of at least one kink soliton is topologically protected and in general, there must always be an odd number. Equation (6) can be solved exactly to give a solution in terms of elliptic functions as

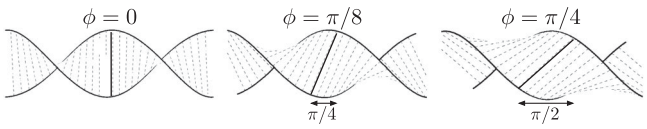

FIG. 3. The ruled approximation used to find the shape of the kink soliton. The surface consists of straight lines connecting points on one boundary helix to those with a phase difference of 2ϕ on the opposite boundary helix. The surface is only minimal for $\phi = 0$, which gives the helicoid, increasing $|\phi|$ decreases the quality of the approximation.

$$\phi = \pm\sqrt{\frac{4m^2\lambda - b^2}{2\lambda}}\,\mathrm{sn}\left(b(z-a), \frac{4m^2\lambda}{b^2} - 1\right), \quad (7)$$

where $m^2 = -\beta/(2\lambda)$, $\lambda = \gamma/(2\delta)$ and a, b are constants. For a n (n odd) kink solution, the value of the constant b is found by satisfying the boundary conditions $\phi(z) = -\phi(z + q\pi)$, which can be written as

$$\frac{q\pi}{n} = \frac{2}{b}K\left(\frac{4m^2\lambda}{b^2} - 1\right), \quad (8)$$

where $K(x)$ is the complete elliptic integral of the first kind. Focusing on the lowest area $n = 1$ solution, note that motion of the soliton along the strip that keeps the boundary fixed can be generated by varying a and is a zero energy deformation of the surface. A full circuit of the strip, corresponding to a translation of the soliton by $q\pi$, sends $\phi \to -\phi$ and illustrates the kink and antikink equivalence in the nonorientable case. Indeed, the ground state manifold in the nonorientable case is a circle, a double cover of the original domain in (6).

The system given by (7) has two length scales: the length of the circle, $q\pi$, and the preferred width of the soliton, $1/\sqrt{2\lambda}m$. If $q\pi\sqrt{2\lambda}m \gg 1$, which can be satisfied by having a large number of twists in the helical boundary (q large), then the solutions on the circle are well-approximated by the standard kink solution

$$\phi(z) = \pm m\tanh(\sqrt{2\lambda}mz). \quad (9)$$

Note that in the vicinity of $\bar{\rho}$, $\sqrt{2\lambda}m \sim (\rho - \bar{\rho})^{1/2}$ and so this approximation requires, for finite q, that ρ is sufficiently above the critical value. As seen in Fig. 1, this approximate solution shows a close correspondence to the experimental structure.

As $\rho \to \infty$, the width of the soliton has a limit of $\sqrt{2}$. While this limit is outside the range of applicability of our approximations, from a topological perspective, one can show that a finite limiting width must exist. The existence of the defect implies that the curve $x = y = 0$, and any isotopic curve lying in the interior of the helical frame, must intersect the surface once. As such, when projected onto the $z = 0$ plane, the soliton must span a disc of radius ρ. The smallest z interval within which the boundary of this disc can be mapped onto the boundary of the helicoid is π, giving a lower bound for soliton width. Using surface evolver [30], surfaces attaining close to this limit can be found for $\rho \gtrapprox 3$. We note that a fuller discussion of the equilibrium shape of the physical system would be to consider a competition between the surface tension of the film and the elastic energy of the boundary wire, the so-called Euler-Plateau problem [31].

The Lagrangian (6) has a continuous translational symmetry, corresponding to the continuous screw symmetry of the helicoidal frame. This leads to the presence of a Goldstone mode [25], localized to the defect, and ultimately allows it to move. In physical realizations of these systems, the boundary curve typically does not possess this symmetry, and the location and motion of the soliton is driven by the inhomogeneities in the boundary. An example of this is shown in Fig. 2(b), and more generally, the bent helicoids, where the axis is circular. In this case, the continuous screw symmetry is broken to a discrete q-fold rotational symmetry, leading to q preferred locations for the defect. Experimental, numerical, and theoretical [32] results all indicate that on a circular frame the defect is located in such a way that the line in the center of the defect points towards the center of the circle, as shown in Fig. 2(b).

Making the axis circular allows us to specify where the defect will be up to the q-fold degeneracy, but does not allow for easy manipulation of its position. To control the defect's location, and induce motion, we can construct simple deformations of a straight helicoid. Moving the helicoid along its local axis in the periodic domain can be achieved by setting the boundary curves to $(\rho\cos z, \rho\sin z, z + g(z) + h(z))$ and $(-\rho\cos z, -\rho\sin z, z + g(z) - h(z))$, where $z \in [0, q\pi)$ and the shifts are determined by the functions g and h, where $g(z)$ controls the local pitch of the helicoid, given by $1 + g'$, and $h(z)$ the local phase difference between points on boundary curves of equal height. In the nonorientable case (q odd) continuity demands that $g(z + q\pi) = g(z)$ and $h(z + q\pi) = -h(z)$. A deformation with $h(z)$ constant and $g(z) = 0$ does not distort the boundary curves, and thus costs no elastic energy locally. For an orientable helicoid, $h(z)$ controls which of the two possible ribbons are energetically favorable; in the ruled approximation, setting h leads to linear and cubic terms in (6) such that ϕ is favored to have the opposite sign from h. In the nonorientable case, h must satisfy $h(z) = -h(z + q\pi)$, so cannot be constant everywhere and must contain an odd number of zeros. These zeros represent places where the preferred ribbon type changes from one to another and are consequently favored places for defects to be located. Figure 1 shows a photograph of a defect in a soap film on a straight helical frame. If d_i denotes the distance between two points on the boundary curves of the same phase, as indicated in Fig. 1 then $d_i = \pi \pm [h(\tilde{z}) + h(\tilde{z} + \pi)]$ with the sign alternating between plus and minus on consecutive intervals and where $\tilde{z}$ is the value of z on the first measuring point. From the image, we can see that to the left of the soliton $d_{2n} > d_{2n\pm1}$, whereas to the right $d_{2n} < d_{2n\pm1}$, indicating that the sign of h has changed and the defect is located at a zero of the function h. In this way, by controlling the shape of the boundary through the function h, one can control the location of the defect. In the Supplemental Material [29], we show videos of boundary deformations creating motion of the soliton through this mechanism. This type of soliton, or kink, motion offers a potential prototype for further study of minimal surface dynamics and interconversion.

We would like to thank D. Michieletto, D. Papavassiliou, M. Contino, J. A. Cohen, M. Polin, V. Kantsler, M. S. Turner, G. Rowlands, H. K. Moffatt, and R. B. Kusner for useful discussions. This work was supported in part by the UK EPSRC through Grant No. A.MACX.0002 (TM and GPA) and an EPSRC Established Career Fellowship (R. E. G. and A. I. P.). TM also supported by a University of Warwick Chancellor's International Scholarship and by a University of Warwick IAS Early Career Fellowship.

[1] J. A. F. Plateau, *Statique Experimentale et Theorique des Liquides Soumis aux Seules Forces Moleculaires* (Gauthier-Villiard, Paris, 1873).
[2] A. H. Schoen, Reflections concerning triply-periodic minimal surfaces, Interface Focus **2**, 658 (2012).
[3] W. Longley and T. J. McIntosh, A bicontinuous tetrahedral structure in a liquid-crystalline lipid, Nature (London) **303**, 612 (1983).
[4] S. T. Hyde, S. Andersson, B. Ericsson, and K. Larsson, A cubic structure consisting of a lipid bilayer forming an infinite periodic minimum surface of the gyroid type in the glycerolmonooleat-water system, Z. Kristallogr. **168**, 213 (1984).
[5] R. D. Kamien and T. C. Lubensky, Minimal Surfaces, Screw Dislocations, and Twist Grain Boundaries, Phys. Rev. Lett. **82**, 2892 (1999).
[6] E. A. Matsumoto, C. D. Santangelo, and R. D. Kamien, Smectic pores and defect cores, Interface Focus **2**, 617 (2012).
[7] Z. A. Almsherqi, T. Landh, S. D. Kohlwein, and Y. Deng, Chapter 6 Cubic Membranes: The Missing Dimension of Cell Membrane Organization, Int. Rev. Cell Mol. Bio. **274**, 275 (2009).
[8] G. E. Schröder-Turk, S. Wickham, H. Averdunk, F. Brink, J. D. Fitz Gerald, L. Poladian, M. C. J. Large, and S. T. Hyde, The chiral structure of porous chitin within the wing-scales of *Callophrys rubi*, J. Struct. Biol. **174**, 290 (2011).
[9] N. J. Hitchin, Monopoles and geodesics, Commun. Math. Phys. **83**, 579 (1982).
[10] N. J. Hitchin, Monopoles, minimal surfaces and algebraic curves, in *Séminaire de Mathématiques Supérieures*, Vol. 105 (Presses de l'Université de Montréal, Montreal, 1987).
[11] D. Fischer-Colbrie and R. Schoen, The structure of complete stable minimal surfaces in 3-manifolds of non-negative scalar curvature, Commun. Pure Appl. Math. **33**, 199 (1980).
[12] S. A. Cryer and P. H. Steen, Collapse of the soap-film bridge: quasistatic description, J. Colloid Interface Sci. **154**, 276 (1992).
[13] Y. J. Chen and P. H. Steen, Dynamics of inviscid capillary breakup: collapse and pinchoff of a film bridge, J. Fluid Mech. **341**, 245 (1997).
[14] R. E. Goldstein, H. K. Moffatt, A. I. Pesci, and R. L. Ricca, Soap-film Möbius strip changes topology with a twist singularity, Proc. Natl. Acad. Sci. U.S.A. **107**, 21979 (2010).
[15] R. E. Goldstein, J. McTavish, H. K. Moffatt, and A. I. Pesci, Boundary singularities produced by the motion of soap films, Proc. Natl. Acad. Sci. U.S.A. **111**, 8339 (2014).
[16] A. I. Pesci, R. E. Goldstein, G. P. Alexander, and H. K. Moffatt, Instability of a Möbius Strip Minimal Surface and a Link with Systolic Geometry, Phys. Rev. Lett. **114**, 127801 (2015).
[17] R. Courant, Soap film experiments with minimal surfaces, Am. Math. Mon. **47**, 167 (1940).
[18] A. Boudaoud, P. Patrício, and M. Ben Amar, The Helicoid versus the Catenoid: Geometrically Induced Bifurcations, Phys. Rev. Lett. **83**, 3836 (1999).
[19] W. P. Su, J. R. Schrieffer, and A. J. Heeger, Solitons in Polyacetylene, Phys. Rev. Lett. **42**, 1698 (1979).
[20] W. P. Su, J. R. Schrieffer, and A. J. Heeger, Soliton excitations in polyacetylene, Phys. Rev. B **22**, 2099 (1980).
[21] A. J. Heeger, S. Kivelson, J. R. Schrieffer, and W. P. Su, Solitons in conducting polymers, Rev. Mod. Phys. **60**, 781 (1988).
[22] C. L. Kane and T. C. Lubensky, Topological boundary modes in isostatic lattices, Nat. Phys. **10**, 39 (2014).
[23] B. G. Chen, N. Upadhyaya, and V. Vitelli, Nonlinear conduction via solitons in a topological mechanical insulator, Proc. Natl. Acad. Sci. U.S.A. **111**, 13004 (2014).
[24] N. S. Manton and P. M. Sutcliffe, *Topological Solitons* (Cambridge University Press, Cambridge, 2004).
[25] T. Vachaspati, *Kinks and Domain Walls: An Introduction to Classical and Quantum Solitons* (Cambridge University Press, Cambridge, 2010).
[26] R. Neel, *Lectures on Minimal Surfaces*, Vol. 1 (Cambridge University Press, Cambridge, 1989).
[27] W. H. Meeks III and M. Weber, Bending the helicoid, Math. Ann. **339**, 783 (2007).
[28] P. Mira, Complete minimal Möbius strips in $\mathbb{R}^n$ and the Björling problem, J. Geometry Phys. **56**, 1506 (2006).
[29] See Supplemental Material at http://link.aps.org/supplemental/10.1103/PhysRevLett.117.017801 for additional details on instabilities in minimal surfaces and the Jacobi fields of the periodic helicoids, the ruled surface approximation described in the main text, and descriptions of accompanying videos of experimentally created solitons.
[30] K. A. Brakke, The surface evolver, Exp. Math. **1**, 141 (1992).
[31] L. Giomi and L. Mahadevan, Minimal surfaces bounded by elastic lines, Proc. R. Soc. A **468**, 1851 (2012).
[32] This can be done by expanding in the reciprocal radius of the axis circle and treating the resulting modified one dimensional Lagrangian with perturbation theory.